

## Journal Pre-proof

Association between carotid atherosclerosis and brain activation patterns during the Stroop task in older adults: an fNIRS investigation

Sarah A. Mason, Lamia Al Saikhan, Siana Jones, Sarah-Naomi James, Heidi Murray-Smith, Alicja Rapala, Suzanne Williams, Carole Sudre, Brian Wong, Marcus Richards, Nick C. Fox, Rebecca Hardy, Jonathan M. Schott, Nish Chaturvedi, Alun D. Hughes



PII: S1053-8119(22)00421-9  
DOI: <https://doi.org/10.1016/j.neuroimage.2022.119302>  
Reference: YNIMG 119302

To appear in: *NeuroImage*

Received date: 4 January 2022  
Revised date: 7 May 2022  
Accepted date: 9 May 2022

Please cite this article as: Sarah A. Mason, Lamia Al Saikhan, Siana Jones, Sarah-Naomi James, Heidi Murray-Smith, Alicja Rapala, Suzanne Williams, Carole Sudre, Brian Wong, Marcus Richards, Nick C. Fox, Rebecca Hardy, Jonathan M. Schott, Nish Chaturvedi, Alun D. Hughes, Association between carotid atherosclerosis and brain activation patterns during the Stroop task in older adults: an fNIRS investigation, *NeuroImage* (2022), doi: <https://doi.org/10.1016/j.neuroimage.2022.119302>

This is a PDF file of an article that has undergone enhancements after acceptance, such as the addition of a cover page and metadata, and formatting for readability, but it is not yet the definitive version of record. This version will undergo additional copyediting, typesetting and review before it is published in its final form, but we are providing this version to give early visibility of the article. Please note that, during the production process, errors may be discovered which could affect the content, and all legal disclaimers that apply to the journal pertain.

© 2022 Published by Elsevier Inc.  
This is an open access article under the CC BY-NC-ND license  
(<http://creativecommons.org/licenses/by-nc-nd/4.0/>)

**Highlights**

- Cognitively normal individuals aged 72 - 73 recruited from a UK-based National Birth Cohort with (n = 33) and without carotid atherosclerosis (n = 33) underwent a Stroop color word task with concurrent assessment of functional near infrared spectroscopy (fNIRS) and hemodynamics.
- Carotid atherosclerosis was associated with a decrease in the extent of brain activation as measured by fNIRS in response to the Stroop test.
- The differences were observed despite no differences in time required to complete the task or number of errors made, or changes in mean arterial pressure or heart rate.
- The results suggest that carotid atherosclerosis is associated with alterations in functional brain activation patterns without impaired Stroop task performance.

# Association between carotid atherosclerosis and brain activation patterns during the Stroop task in older adults: an fNIRS investigation

Sarah A Mason<sup>a,\*</sup>, Lamia Al Saikhan<sup>b</sup>, Siana Jones<sup>a</sup>, Sarah-Naomi James<sup>a, c</sup>, Heidi Murray-Smith<sup>d</sup>, Alicja Rapala<sup>a</sup>, Suzanne Williams<sup>a</sup>, Carole Sudre<sup>a, d, e</sup>, Brian Wong<sup>a</sup>, Marcus Richards<sup>a</sup>, Nick C. Fox<sup>c</sup>, Rebecca Hardy<sup>a</sup>, Jonathan M. Schott<sup>a, d</sup>, Nish Chaturvedi<sup>a</sup>, Alun D Hughes<sup>a,\*</sup>

<sup>a</sup> MRC Unit for Lifelong Health and Ageing at University College London, Department of Population Science and Experimental Medicine, Institute of Cardiovascular Science, 1-19 Torrington Place, London, United Kingdom, WC1E 7HB

<sup>b</sup>Department of Cardiac Technology, College of Applied Medical Sciences, Imam Abdulrahman Bin Faisal University, 2835 King Faisal Street, Damman, Kingdom of Saudi Arabia

<sup>c</sup>Dementia Research Centre, Institute of Neurology, University College London, London, UK

<sup>d</sup>Centre for Medical Image Computing, Department of Computer Science, University College London, London UK

<sup>e</sup>School of Biomedical Engineering, King's College, London

**Abstract.** There is an increasing body of evidence suggesting that vascular disease could contribute to cognitive decline and overt dementia. Of particular interest is atherosclerosis, as it is not only associated with dementia, but could be a potential mechanism through which cardiovascular disease directly impacts brain health. In this work, we evaluated the differences in functional near infrared spectroscopy (fNIRS)-based measures of brain activation, task performance, and the change in central hemodynamics (mean arterial pressure (MAP) and heart rate (HR)) during a Stroop color-word task in individuals with atherosclerosis, defined as bilateral carotid plaques ( $n = 33$ ) and healthy age-matched controls ( $n = 33$ ). In the healthy control group, the left prefrontal cortex (LPFC) was the only region showing evidence of activation when comparing the incongruous with the nominal Stroop test. A smaller extent of brain activation was observed in the Plaque group compared with the healthy controls (1) globally, as measured by oxygenated hemoglobin ( $p = 0.036$ ) and (2) in the LPFC ( $p = 0.02$ ) and left sensorimotor cortices (LMC) ( $p = 0.008$ ) as measured by deoxygenated hemoglobin. There were no significant differences in HR, MAP, or task performance (both in terms of the time required to complete the task and number of errors made) between Plaque and control groups. These results suggest that carotid atherosclerosis is associated with altered functional brain activation patterns despite no evidence of impaired performance of the Stroop task or central hemodynamic changes.

**Keywords:** functional near infrared spectroscopy (fNIRS), neurovascular coupling, Stroop task, cognitive function.

\*Sarah A. Mason, [s.mason@ucl.ac.uk](mailto:s.mason@ucl.ac.uk) \*Alun D. Hughes, [alun.hughes@ucl.ac.uk](mailto:alun.hughes@ucl.ac.uk)

## 1 Introduction

- 1 A variety of cardiovascular risk factors or cardiovascular disease biomarkers are associated with
- 2 impaired cognitive function. For example, carotid stenosis,<sup>1</sup> increased arterial stiffness,<sup>2</sup> poorer
- 3 cardiac function,<sup>3</sup> and carotid atherosclerosis (defined as a thickening and hardening of arteries
- 4 due to a buildup of plaque in the lumen)<sup>4</sup> have been associated with poor performance in tests

5 of attention, memory, processing speed, and executive function. Furthermore, there is evidence  
6 suggesting that cardiovascular risk factors are not only associated with cognitive impairment and  
7 Alzheimer's disease (AD), but may in fact precede and/or accelerate the onset of neurodegenera-  
8 tion.<sup>5-9</sup> It has been posited that vascular dysfunction or damage arising from cardiovascular risk  
9 factors can lead to chronic hypoperfusion and ischemia, impaired cerebral blood flow regulation,  
10 and disruption to the blood-brain barrier.<sup>5</sup> According to the Vascular Hypothesis,<sup>10,11</sup> these hemo-  
11 dynamic disturbances not only cause direct brain injury, but can initiate cerebral angiopathy by  
12 triggering over-production and reduced clearance of amyloid  $\beta$ -protein, thereby leading to deficits  
13 in cognitive domains such as executive function and memory, and potentially resulting in overt  
14 dementia.<sup>5,7,8,12</sup>

15 Atherosclerosis underlies the majority of cardiovascular diseases and is relevant to cogni-  
16 tion given that it is not only associated with dementia<sup>13</sup> and an increase in cerebral amyloid  
17 deposits,<sup>14,15</sup> but could be a potential mechanism through which cardiovascular disease directly  
18 impacts brain health.<sup>8</sup> To better understand the potential role of atherosclerosis in cognitive im-  
19 pairment, we sought to compare (1) cognitive performance, (2) central hemodynamic changes,  
20 and (3) patterns of functional brain activity using functional near infrared spectroscopy (fNIRS)  
21 in older adults with and without carotid atherosclerosis during an incongruous Stroop color-word  
22 task.

23 The participants in this work were part of the Insight 46 neuroscience sub-study of the Na-  
24 tional Survey of Health and Development (NSHD). NSHD is an ongoing British birth cohort study  
25 where social, lifestyle, cognitive and physical data from over 5000 individuals born within the same  
26 week in 1946 has been assessed over the course of the participants' lives.<sup>16-18</sup> A sub-sample of 502  
27 NSHD participants volunteered for the Insight 46 study, which is designed to explore prelini-

28 cal dementia and the causes/consequences of cerebrovascular amyloid pathology on brain health  
29 through a battery of clinical, neuropsychological, imaging, biomarker, genetic, and vascular as-  
30 sessments.<sup>19,20</sup> Insight 46 provides a powerful opportunity to investigate the mechanisms of early  
31 cognitive decline as many participants in this study (aged 72 - 73) likely exhibit subclinical patho-  
32 physiological changes such as amyloid pathology and atherosclerosis yet have a low risk of overt  
33 dementia.<sup>21</sup>

34 The extensive phenotyping protocol performed as part of the Insight 46 study involves psycho-  
35 metric testing using fNIRS.<sup>20</sup> fNIRS is an optical technique whereby changes in concentration of  
36 oxygenated hemoglobin (O<sub>2</sub>Hb) and deoxygenated hemoglobin (HHb) in the cerebral microvas-  
37 culature of the cortical surface can be detected.<sup>22,23</sup> As fNIRS is non-invasive and relatively in-  
38 sensitive to motion, it can be used to evaluate hemodynamic changes arising from neurovascular  
39 coupling (NVC) during a variety of cognitive tasks in a naturalistic environment.<sup>24,25</sup> NVC refers  
40 to the localised increase in blood flow that occurs in response to a cognitive stimulus, and is com-  
41 monly used as a surrogate for neuronal activity.

42 In this work, we assessed fNIRS-based measures of brain activity in older adults during the  
43 Stroop color-word task, which is a well-established method for evaluating executive function,  
44 specifically in the ability to inhibit automatic responses.<sup>26-28</sup> The degree of Stroop interference  
45 (both in terms of response time and the number of errors made) not only increases as a function of  
46 normal ageing,<sup>29</sup> but is exacerbated by conditions such as cognitive impairment and dementia.<sup>30-32</sup>

47 Here, we use the presence of ultrasound-diagnosed bilateral carotid plaques as an indicator of  
48 moderately severe atherosclerotic burden, and assess whether there are any differences in perfor-  
49 mance, hemodynamics, and/or brain activation patterns in atherosclerotic individuals compared  
50 with age-matched controls. We hypothesize that atherosclerotic individuals will perform signifi-

51 cantly worse than the healthy controls on the Stroop task in terms of both time to complete the task  
52 and the number of errors made. NVC is identified in regions where there is a concurrent increase  
53 in O2Hb concentration and decrease in Hb concentration. We aim to compare fNIRS-measures  
54 of changes in O2Hb and Hb between groups between corresponding anatomical brain regions to  
55 determine the strength and location of NVC. We hypothesize that the presence of bilateral carotid  
56 plaques will be associated with a significant reduction in NVC primarily in the prefrontal cortices  
57 when comparing the incongruous with the nominal Stroop test. .

## 58 **2 Methods**

### 59 *2.1 Participant recruitment*

60 Participants were selected from 184 participants (aged 72 - 73) who attended an Insight 46 clinic  
61 between October 2018 - March 2020. Research Ethics Committees in England and Scotland  
62 provided approval for NSHD.<sup>16,18,19,33</sup> The National Research Ethics Service Committee London  
63 (REC reference 14/LO/1173) approved the Insight 46 sub-study. All participants provided written  
64 informed consent to participate and for their data to be stored. Exclusion criteria for the study  
65 included: a Mini-Mental State Exam (MMSE) below 24, established cardiovascular disease at age  
66 53, heart attack by the age of 69.

### 67 *2.2 Investigations*

68 The Insight 46 protocols have been previously described.<sup>20</sup> All participants completed a health  
69 and lifestyle questionnaire and underwent measurements of height and weight, blood pressure, and  
70 blood tests. Cholesterol/high density lipoprotein (HDL) ratio was calculated for each participant  
71 from the most recently available data from the NSHD database. The MMSE score from each

72 participant was also obtained from the most recently available data from the NHSD database to  
73 confirm that participants had normal cognitive function. An EPIQ 7G ultrasound scanner (Philips  
74 Healthcare, Andover MA, USA) with a linear array transducer (L12-3) was used to check for the  
75 presence of plaques in the left and right carotid arteries. A plaque was defined as a focal structure  
76 that encroaches into the arterial lumen by at least 0.5 mm or 50% of the surrounding intima-media  
77 thickness or a region of intima-media thickness  $>1.5$  mm.<sup>34</sup> Echocardiography was performed  
78 using an EPIQ 7G ultrasound scanner with an X5-1 transducer. A 3-lead electrocardiogram (ECG)  
79 was recorded concurrently with all ultrasound examinations. In addition, a standard 12-lead resting  
80 ECG was performed in the supine position. All abnormal findings (presence of carotid plaques,  
81 dilated atria, atrial fibrillation, left bundle branch block, aortic valve calcification, left ventricular  
82 hypertrophy, low voltage QRS etc.) were recorded in the electronic case report form.

83 Findings on vascular ultrasound, echocardiography, and 12-lead electrocardiography (ECG)  
84 were used to categorize the study participants based on their cardiovascular health at the time of  
85 their second Insight 46 clinic visit. Participants were tagged with at least one label as shown in  
86 Table 1 depending on the number and type of incidental findings from the cardiovascular assess-  
87 ment. Participants with label 0 (no incidental findings) were classified as 'Healthy' and participants  
88 with label 3 (more severe atherosclerosis, with plaque detected on both the left and right carotid  
89 artery) were categorized into the 'Plaque' group. Note that participants with unilateral plaques  
90 were excluded from further analysis.

### 91 *2.3 Stroop color-word testing protocol*

92 A verbal Stroop color-word task was performed. Though there are different versions of the Stroop  
93 test, the basic concept is to measure the accuracy and speed with which one can identify the color

**Table 1** - Labels used for participant categorization based on incidental findings from the cardiovascular assessment

Label	Definition
0	No incidental findings
1	Carotid plaque (left side only)
2	Carotid plaque (right side only)
3	Carotid plaques (both sides)
4	Abnormal ECG
5	Other

94 of a word printed in ink mismatched to the meaning of the color (i.e. the word ‘blue’ printed in  
 95 green ink). As language is a powerful distractor, there is a natural delay in response time in this  
 96 task compared with identifying the color of non-words (such as ‘XXXXX’ printed in green ink, for  
 97 example). Our implementation of the Stroop task consisted of three blocks, with each block pre-  
 98 ceded and followed by a 60-second baseline/recovery period where the participant stared straight  
 99 ahead at a black poster. All blocks were presented on white A4 laminated sheets of paper held  
 100 upright by a free-standing clipboard to avoid a downward head-tilt whilst reading. The description  
 101 of each block of the Stroop task is described below:

- 102 • Block 1 - **Nominal**: Participants read aloud 100 words (spelling either ‘blue’, ‘red’, or  
 103 ‘green’) printed in black ink in five evenly spaced columns on the page
- 104 • Block 2 - **Congruous**: Participants read aloud colors of 100 ‘XXXXX’ (printed in either  
 105 blue, red, or green ink) displayed in five evenly spaced columns on the page
- 106 • Block 3 - **Incongruous**: Participants read aloud the color (red, blue or green ink) of 100  
 107 words (spelling ‘red’, ‘green’, or ‘blue’), where the color of the word was mismatched to the  
 108 meaning of the word itself. The words were displayed in five evenly spaced columns on the



109 page.

110 The number of errors made and time required to complete each Stroop block were recorded to  
111 quantify task performance.

#### 112 *2.4 Hemodynamic and fNIRS monitoring during the Stroop task*

113 Throughout the duration of the Stroop task, cerebral hemodynamics were monitored with an 18-  
114 channel, dual-wavelength (760 and 850 nm) continuous wave Brite 24 fNIRS device (Artinis Med-  
115 ical Systems, BV, Zetten, The Netherlands). This device had 16 long separation channels (where  
116 the source and detector were separated by 3 cm) arranged in quadrants approximately over the  
117 left and right prefrontal cortex (LPFC/RPFC) and the left and right motor/somatosensory cortices  
118 (LMC/RMC). This device also had 2 short separation channels (where the source and detector were  
119 separated by 1 cm) placed on the left and right PFC. See Figure 1 for an illustration of channel  
120 positioning. The sampling frequency of this device was 10 Hz. The investigator positioned the cap  
121 symmetrically on the participant's head with the brim approximately 1 cm above the eyebrows,  
122 and secured the position of the cap using the chin strap. A Polhemus Patriot Device (Polhemus,  
123 Colchester, VT, USA) was used to determine the position of each source and detector with re-  
124 spect to anatomical landmarks of the head based on the international 10/20 system.<sup>35</sup> The operator  
125 tagged the position of the nasion, inion, left preauricular point, right preauricular point, top of the  
126 head along the mid-sagittal plane (Cz), each source, and each detector using the electromagnetic  
127 Polhemus sensor. These positions were converted from real space to the Montreal Neurological  
128 Institute (MNI) stereotaxic coordinate system automatically in the software used to interface with  
129 the Brite 24 (Oxysoft, Artinis Medical Systems, BV, Zetten, the Netherlands).

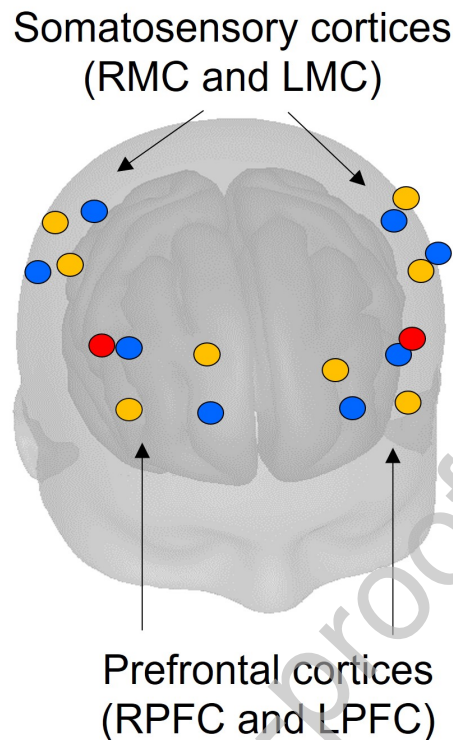


**Fig 1** An example of the channel position of the Brite 24 cap obtained with the Pohemus digitization. Sources are shown in orange (long separation channels) and red (short separation channels). Detectors are shown in blue. Note that the sources and detectors are arranged in quadrants over the left and right somatosensory cortices and prefrontal cortices.

130 Changes in beat-to-beat peripheral mean arterial pressure (MAP) and heart rate (HR) were also  
 131 monitored during the Stroop task using a Finometer (Finapres Medical Systems BV, the Nether-  
 132 lands) placed on the finger cuff on either the index finger or middle finger of the non-dominant hand  
 133 according to the manufacturer's instructions. Finometer readings were synchronized with fNIRS  
 134 readings using electronic markers to indicate the start and end of each Stroop and baseline/recovery  
 135 block.

### 136 2.5 fNIRS signal processing pipeline

137 All analyses were performed in Matlab<sup>®</sup> (2021a) using the SPM-fNIRS toolbox developed by  
 138 the NeuroImaging Tools & Resources Collaboratory (NITRC).<sup>36</sup> This software enabled statistical

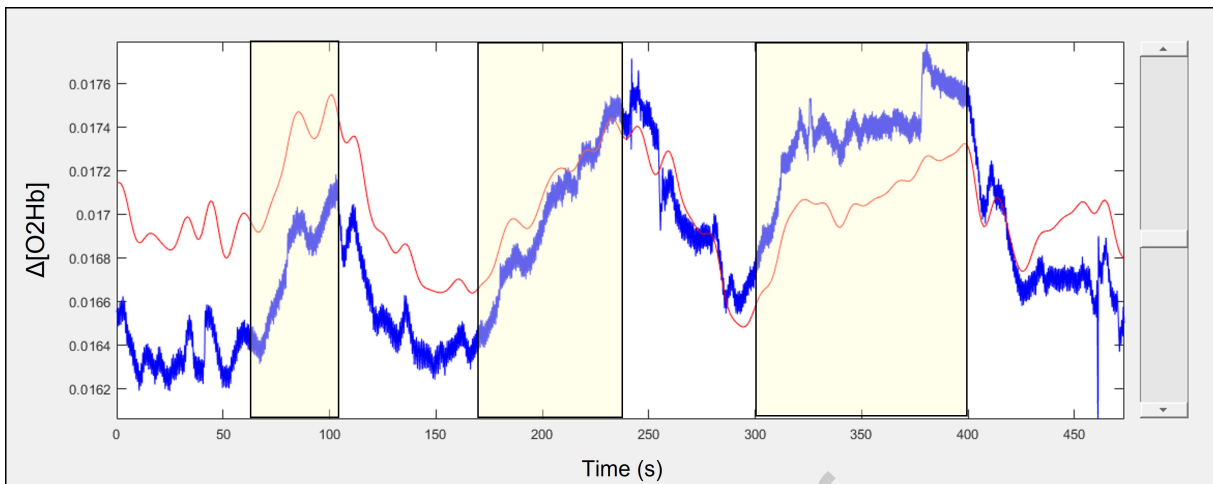


**Fig 2** An example of unprocessed (blue) and fully processed (red) fNIRS data obtained from a participant performing the verbal Stroop task. The trace shown is  $\Delta\text{O}_2\text{Hb}$  in units of mol/L. The stimulus periods (Stroop blocks 1, 2, and 3) are indicated by the yellow rectangles superimposed over the fNIRS traces.

139 parametric mapping of fNIRS data using SPM12 software.

#### 140 2.5.1 Temporal preprocessing and channel rejection

141 fNIRS Intensity data from each channel was converted into  $\Delta\text{O}_2\text{Hb}$  and  $\Delta\text{HHb}$  using the Modified  
 142 Beer Lambert Law and differential pathlength factors (DPF) of 7.4 and 6.4 for the 760 nm and  
 143 850 nm wavelengths respectively. These DPFs were calculated automatically in the SPM-fNIRS  
 144 software using the age-dependent general equation for the DPF derived by Scholkmann and Wolf.<sup>37</sup>  
 145 Motion artefacts were corrected using the Motion Artifact Reduction Algorithm (MARA) with the  
 146 default values of 1, 3, and 5 accepted for the moving window length (L), threshold factor-motion  
 147 detection (th) and smoothing factor motion artifact ( $\alpha$ ) parameters respectively.<sup>38</sup> A band-stop filter  
 148 with cut-off frequencies of 0.1 and 2 Hz was applied to remove physiological noise. The data were  
 149 then downsampled to 1 Hz and linear de-trended using a discrete cosine transform (DCT) with  
 150 a cutoff of 160 seconds. An example channel from a study participant before and after temporal  
 151 preprocessing is shown in Figure 2.

152 The frequency spectrum of the  $\Delta O_2Hb$  for each channel (before filtering) was visually assessed  
153 in the SPM-fNIRS temporal preprocessing GUI to check for a peak at around 1 Hz corresponding  
154 to the cerebrovascular pulsatility arising from the heartbeat. This is a well-established indicator of  
155 fNIRS signal quality as it demonstrates good optical coupling has been achieved.<sup>39</sup> Any trace with  
156 a very small or non-existent peak was visually inspected further in the time domain to confirm  
157 poor data quality. Any trace with poor optical coupling (arising from either an over-saturation  
158 of ambient light or poor contact with the participant's scalp) or completely corrupted by motion  
159 artefacts was rejected and not analysed further. Each participant was given an overall fNIRS signal  
160 quality rating based on the following criteria:

161 1. **Unacceptable:** Over half of the channels were rejected, and/or  $O_2Hb$  and  $HHb$  were suspi-  
162 ciously correlated due to motion artefacts not adequately corrected for by the MARA algo-  
163 rithm

164 2. **Acceptable:** At least half of the channels retained, with zero to minor detectable artefacts

165 Only participants with a rating of 'Acceptable' were considered for further analysis.

### 166 2.5.2 Model Specification and Estimation

167 A general linear model (GLM) was used to analyse the temporally preprocessed  $O_2Hb$  and  $HHb$   
168 fNIRS signals. The GLM is shown in Equation 1,<sup>22,24,40</sup> where  $Y$  is the measured fNIRS signal  
169 after processing,  $X$  is the design matrix,  $\beta$  is the vector of weights of each regressor in the design  
170 matrix, and  $\epsilon$  is the error. The Model Specification routine in SPM-fNIRS was used to (1) correct  
171 for serial autocorrelations in the fNIRS data using a first order autoregressive (AR(1)) plus white  
172 noise model<sup>41,42</sup> and (2) construct the design matrix, which consisted of:

- 173 1. A task regressor for each of the three Stroop blocks modelled using the canonical hemo-  
 174 dynamic response function (HRF) convolved with the box car function corresponding to  
 175 individual task duration with time and dispersion derivatives to allow for the peak and width  
 176 of the response to vary by plus or minus a second, respectively.<sup>43</sup>
- 177 2. The left and right short separation channels (after preprocessing as described in Section 2.5)  
 178 to remove extracerebral contamination.<sup>22,44</sup>
- 179 3. A constant to model the signal mean.

$$Y = X \cdot \beta + \epsilon \quad (1)$$

180 The  $\beta$  coefficients were solved for on a channel by channel basis using the Model Estimation  
 181 routine in SPM-fNIRS.

## 182 2.6 Evaluation of hemodynamic effects

183 Equation 2 indicates how channel-wise T statistics were calculated given a contrast vector  $c$  and  
 184 the covariance of the  $\beta$  coefficients (see equation 3) calculated using the GLM.<sup>40</sup> The nominal  
 185 Stroop task was chosen as our control as the experimental conditions were identical to the incon-  
 186 gruous Stroop task (i.e. reading and speaking aloud), but the PFC was not activated as this task is  
 187 considered an ‘automatic’ process. We therefore assessed whether there was significantly greater  
 188 evidence of NVC in the incongruous Stroop task (Block 3) compared to the nominal Stroop task  
 189 (Block 1) by setting the contrast vector values to 1 and -1 for the Block 3 task regressor and Block  
 190 1 task regressor, respectively.

$$T = c \cdot \beta / \sqrt{c \cdot Cov_b \cdot c^T} \quad (2)$$

$$Cov_{\beta} = (X^T \cdot X)^{-1} \cdot \sigma^2 \quad (3)$$

## 191 2.7 Statistical Analyses

### 192 2.7.1 Stroop performance

193 The two performance metrics considered were: (1) time required to complete the incongruous  
194 Stroop task and (2) the number of errors made. Data were reported as medians and nonparametric  
195 95% CIs. Differences in both of these performance metrics between the Healthy and Plaque group  
196 were determined using a Mann-Whitney U test.

### 197 2.7.2 Central hemodynamics during Stroop task

198 Data were reported as means  $\pm$  SD. Student's t-tests were used to test for differences between  
199 the Healthy and Plaque groups in the change in MAP and HR during the incongruous Stroop task  
200 relative to the preceding baseline period.

### 201 2.7.3 Cerebral fNIRS during Stroop task

202 The t statistic maps generated for each participant for O2Hb and HbB were subdivided into four  
203 anatomical regions as shown in Figure 3: (1) the left prefrontal cortex (LPFC), (2) the right pre-  
204 frontal cortex (RPFC), (3) the left sensorimotor cortices (LMC), and (4) the right sensorimotor  
205 cortices (RMC). In addition to comparing the overall activation between the Healthy and Plaque  
206 groups in the incongruous relative to the nominal condition, we postulated a priori that there would  
207 be effect modification by anatomical region as we expect minimal activation in the sensorimotor  
208 regions, high activation in the prefrontal regions, and a potential hemispheric effect depending on

209 the dominant hand of the participant. Therefore, the mean T statistic for each region in the incon-  
210 gruous relative to the nominal condition was computed for each participant and was used as the  
211 outcome variable in a robust linear mixed effects (LME) model with anatomical region and group  
212 (Healthy vs. Plaque) as fixed effects and participant ID as a random effect for O2Hb and HbB  
213 separately. The LME analysis was performed using Stata 17 (StataCorp. 2021. Stata Statistical  
214 Software: Release 17. College Station, TX: StataCorp LLC.), other statistical analyses were per-  
215 formed using Matlab 2021a. The RMC was used as the contrast region in the LME model, as we  
216 expect this region to have the lowest level of NVC during the Stroop task because (a) the Stroop  
217 task is not designed to activate motor functions and (b) the right hemisphere may be less dominant  
218 given the handedness of the majority of the participants. The Huber White Sandwich estimator  
219 was used to improve estimates of standard error given the heteroskedasticity of the data. Statistical  
220 significance was assigned using the conventional threshold of  $p < 0.05$ .

### 221 **3 Results**

#### 222 *3.1 Participant characteristics*

223 102 out of 184 fNIRS datasets received a rating of 2 (acceptable quality), and were therefore  
224 considered for further analysis. Of these 102 participants, 33 participants had no incidental findings  
225 and were included in the Healthy group and 33 participants had plaque on both the left and right  
226 carotid arteries and were included in the Plaque group. Note, the groups were not planned to be  
227 matched 1:1, and it is coincidental that there were 33 participants exactly in each group. Table  
228 [2](#) summarizes the sex, handedness, and other cardiovascular health phenotypes assessed for the  
229 participants within each group. There were significantly more men in the Plaque group ( $p =$   
230  $0.007$ ), but otherwise the two groups were similar.

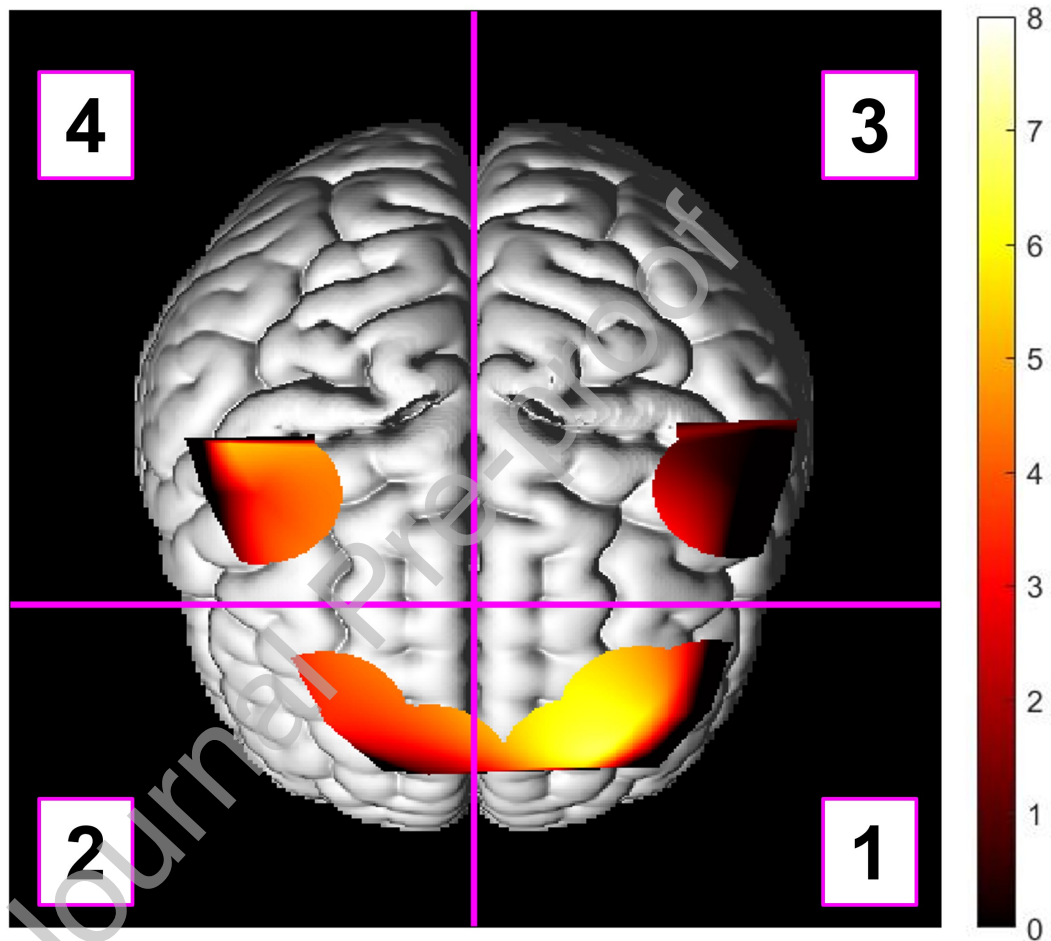


**Fig 3** An example of how the t statistic map superimposed over a rendered brain was subdivided into the four anatomical regions used in the statistical analysis. Region 1 = left prefrontal cortex (LPFC), Region 2 = right prefrontal cortex (RPFC), Region 3 = left sensorimotor cortices (LMC), and Region 4 = right sensorimotor cortices(RMC).



**Table 2** Participant characteristics for each group.

	<b>Healthy (n = 33)</b>	<b>Plaque (n = 33)</b>
<b>Age (mean <math>\pm</math> SD)</b>	73.7 $\pm$ 0.7	73.6 $\pm$ 0.5
<b>Men</b>	12 (36%)	23 (70%)
<b>Right-handed</b>	31 (94%)	30 (91%)
<b>Cardiovascular disease at age 53</b>	0 (0%)	0 (0%)
<b>Type 2 diabetes at age 63</b>	2 (6%)	3 (9%)
<b>Smoking status : Current smokers</b>	0 (0%)	2 (6%)
Ex-smokers	15 (45%)	21 (64%)
Non-smokers	18 (55%)	9 (27%)
Question not answered	0 (0%)	1 (3%)
<b>BMI (age 69 - 71, mean <math>\pm</math> SD)</b>	27.8 $\pm$ 3.5	27.9 $\pm$ 4.2
<b>Systolic blood pressure (age 69 - 71, mean <math>\pm</math> SD)</b>	133.4 $\pm$ 15.2	137.1 $\pm$ 14.6
<b>Diastolic blood pressure (age 69 - 71, mean <math>\pm</math> SD)</b>	74.0 $\pm$ 8.1	75.0 $\pm$ 8.9
<b>Cholesterol/HDL ratio (age 69 - 71, mean <math>\pm</math> SD)</b>	3.4 $\pm$ 1.1	3.3 $\pm$ 1.2
<b>MMSE score (age 69 - 71, mean <math>\pm</math> SD)</b>	29.4 $\pm$ 1.0	29.5 $\pm$ 1.0

### 231 3.2 Performance in Stroop Task

232 The median [95% CI] time to complete the incongruous Stroop task was 104s [98, 122] and 109s  
233 [97, 133] for the Healthy and Plaque groups respectively. The median [95% CI] number of errors  
234 made during the incongruous Stroop task was 1 [1, 3] and 2 [1, 2] for the Healthy and Plaque  
235 groups respectively. There was no evidence of a difference between the Healthy and Plaque groups  
236 in either the time required to complete the task or the number of errors made ( $p = 0.43$  and  $0.99$ ,  
237 respectively). Both the Healthy and Plaque groups made zero errors in the nominal condition of  
238 the Stroop Task.

### 239 3.3 Central hemodynamics during Stroop task

240 There was no evidence of differences in the change in HR or MAP associated with the incongruous  
241 Stroop test between groups with respect to (1) the baseline period or (2) the nominal Stroop task.

242 (1) The mean  $\pm$  SD change in MAP with respect to the baseline period was  $5.8 \pm 5.1$  mmHg  
243 and  $7.3 \pm 4.1$  mmHg for the Healthy and Plaque groups respectively ( $p = 0.24$ ). The mean  $\pm$  SD  
244 change in HR with respect to the baseline period was  $5.0 \pm 3.5$  beats/min and  $3.7 \pm 2.4$  beats/min  
245 for the Healthy and Plaque groups respectively ( $p = 0.13$ ).

246 (2) The mean  $\pm$  SD change in MAP with respect to the nominal Stroop test was  $5.04 \pm 6.4$  mmHg  
247 and  $6.8 \pm 7.0$  mmHg for the Healthy and Plaque groups respectively ( $p = 0.38$ ). The mean  $\pm$   
248 SD change in HR with respect to the nominal Stroop test was  $0.7 \pm 3.9$  beats/min and  $0.67 \pm 1.7$   
249 beats/min for the Healthy and Plaque groups respectively ( $p = 0.93$ ).

### 250 3.4 Cerebral fNIRS during Stroop task

251 Out of the 1188 channels available for analysis (18 channels times 66 participants), 41 were re-  
252 jected in total. The average number of channels excluded per participant was 0.61.

253 Figure 4 shows the mean t statistic maps for the Healthy and Plaque groups for O2Hb and HHb.  
254 The direction of expected change in response to the stimulus (positive for O2Hb and negative for  
255 HHb) was incorporated into the GLM such that a positive t value corresponds to a greater increase  
256 in O2Hb and a greater decrease in HHb with respect to the nominal condition. Note that there is  
257 evidence of increased O2Hb in response to the incongruous condition in all brain regions in the  
258 Healthy group, and in the RPFc, LPFC, and LMC in the Plaque group (prevalence of t values  $>$   
259 2).

260 The LME coefficient indicating the effect of being categorized into the Plaque group for O2Hb  
261 was -1.13 ( $p = 0.036$ ) which suggests that plaque is associated with a global reduction in O2Hb for  
262 all regions. However, there were no significant differences between individual regions observed in  
263 the LME for O2Hb for (i) all participants regardless of group and (ii) when an interaction between  
264 group and region was included. The output from the LME analysis is given in the Supplementary  
265 Information (S1).

266 In the LME for HHB, the LPFC of all participants (regardless of group) showed a significantly  
267 greater drop in HHB compared to the control region, (coefficient = 0.65,  $p = 0.042$ ). There were  
268 no significant differences between Healthy and Plaque groups ( $p = 0.77$ ), which indicates that no  
269 global reduction in HHB was detected. However, significant reductions in HHB in specific regions  
270 were observed when including an interaction between Group and Region. The LPFC (coefficient  
271 = -1.36,  $p = 0.021$ ) and LMC (coefficient = -1.25,  $p = 0.008$ ) showed significantly a significantly  
272 smaller decrease in HHB in the Plaque group compared to the Healthy group as indicated by the  
273 magenta arrows in Figure 4. The output from the LME analysis for HHB is given in Supplementary  
274 Information S1.

275 Together, the results from O2Hb and HHB suggest that NVC (identified by an increase in O2Hb  
276 and corresponding decrease in HHB) is significantly reduced in the left hemisphere of the brain  
277 of participants in the Plaque group compared to the Healthy group. Additionally, the HHB LME  
278 suggests that general activation in the LPFC is observed for participants in both groups in response  
279 to the incongruous Stroop task.

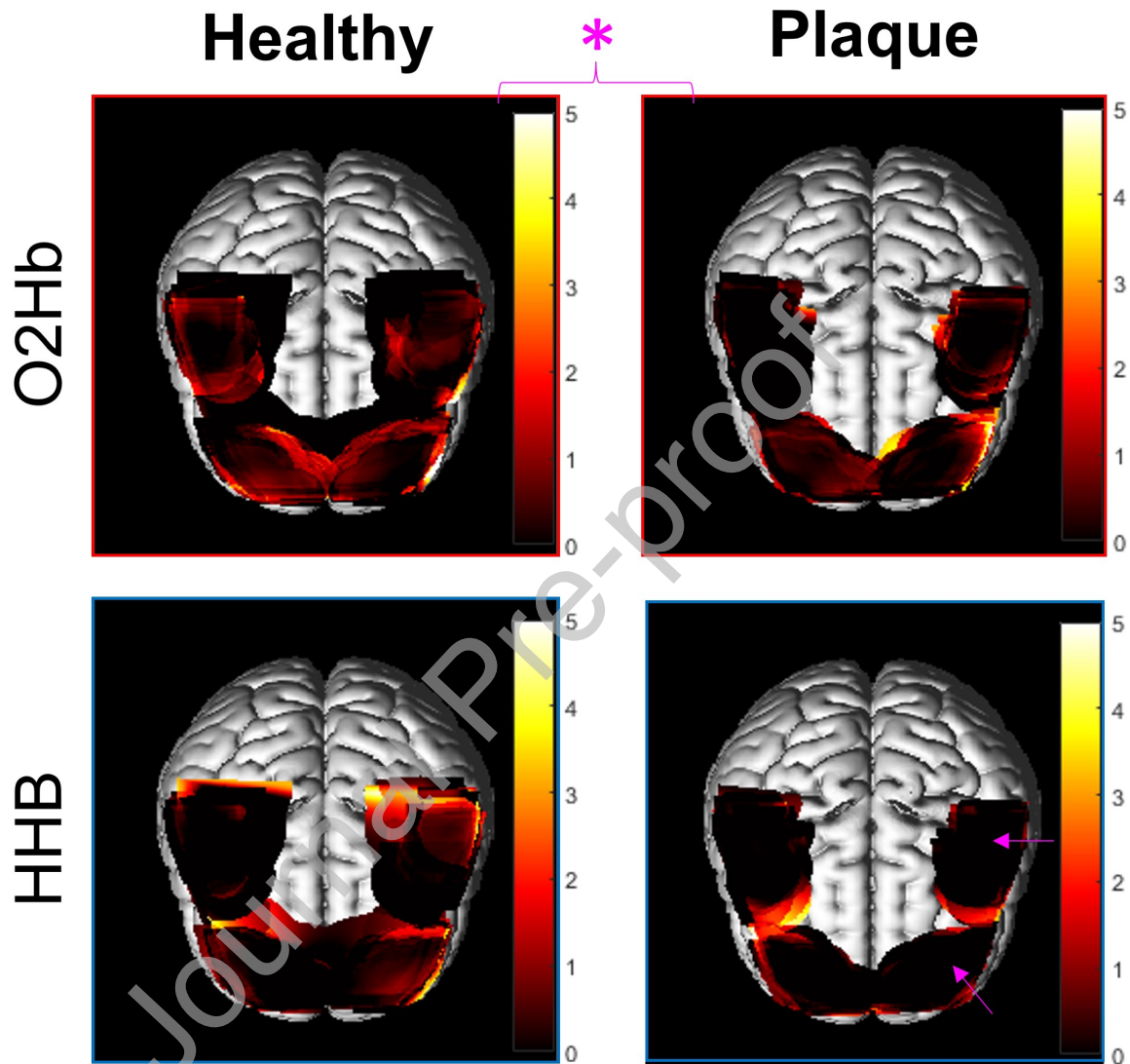


**Fig 4** Shows the mean t statistic maps for each group (Healthy and Plaque) when comparing the incongruous Stroop to the nominal Stroop for oxygenated haemoglobin (O2Hb) and deoxygenated haemoglobin (HHB). The higher the t statistic, the greater evidence of increased change in Hb (rise in O2Hb, fall in Hb), and thus functional brain activity. Note that the average t statistic is significantly lower overall in the Plaque group compared with the Healthy group in O2Hb as indicated by the pink asterisk. Also note the significant reduction in t statistic in the LPFC and LMC in the Plaque group compared with the Healthy group in Hb as indicated by the pink arrows.

## 280 4 Discussion

281 There are various factors contributing to the expected pattern of brain activity during the incongru-  
282 ous Stroop task, such as handedness, age, sex, and brain health.<sup>28,31,45-48</sup> In general, it is widely  
283 accepted that the ability to perform a color-word matching Stroop task requires adequate function  
284 of a fronto-parietal network including the anterior cingulate cortex (ACC), the PFC, and the pari-  
285 etal lobe.<sup>46,49-51</sup> Although the PFC has been shown to be active bilaterally during an incongruous  
286 Stroop task,<sup>31,47,52</sup> there is some evidence suggesting that the left hemisphere may be more active  
287 than the right in young healthy individuals.<sup>53</sup> Due to cap geometry and limitations of fNIRS pen-  
288 etration depth, we were unable to assess activity in the ACC and parietal lobe. We observed that  
289 on average, all regions for all participants (except for the RMC in the Plaque group) demonstrated  
290 an increase in H2Ob in response to the incongruous Stroop task compared with the nominal task  
291 as evidenced by the prevalence of relatively high t values ( $>2$ ) as shown in Figure 4. Given the  
292 global increase in O2Hb, we used HHB (which was more localized) as an arbitrator to determine  
293 which regions likely exhibit evidence of NVC, as an increase in H2Ob alone is not sufficient.<sup>54</sup>  
294 Reassuringly, LME for HHB revealed that all participants had significantly greater decreases in  
295 HHB concentration in the LPFC compared to the RMC ( $p = 0.042$ ). We interpret this to mean that  
296 the LPFC has a significantly greater level of NVC than the RMC (i.e. the control region), which  
297 is broadly consistent with the expected activation pattern of the PFC based on the literature. How-  
298 ever, the HHB LME model did not show significant differences in activation between the RPFC  
299 and RMC. This may be due to an age-related loss of localisation of functional activation, result-  
300 ing in a diffuse, heterogenous, and/or weaker activation in older adults compared with younger  
301 adults.<sup>31,47,55</sup> Indeed, the variability in brain activation patterns between individuals is exempli-

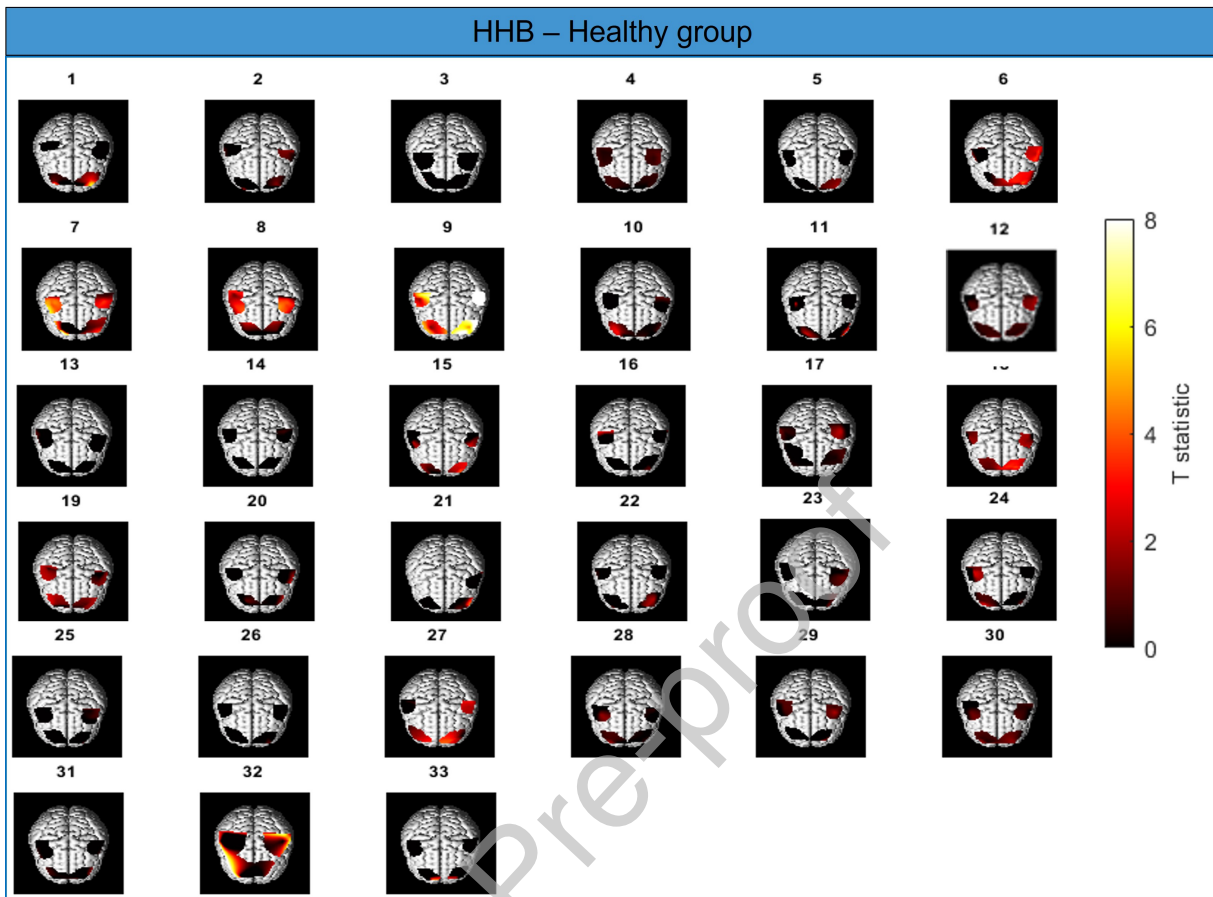


**Fig 5** Individual t statistic maps showing the brain activation pattern for all 33 participants in the Healthy group performing the Stroop task (incongruous vs. null condition). The t statistic is indicated by the colorbar, with brighter colors indicating a high t value and thus greater evidence for NVC.

302 fied in Figure 5. Although some participants retain the ‘model’ activation pattern characterised by  
 303 highly focal regions of activation in the bilateral PFC (e.g. participants 1, 11, 33), the majority  
 304 of participants show a spread in activation (e.g. participants 6, 18, 19, 27) or weak/null global  
 305 activation (e.g. participants 3, 4, 13, 14, 25, 26) which is expected given the age (72 - 73 years)  
 306 of the participants in this study. We did not see any convincing evidence of PFC dominance in the  
 307 O2Hb LME. However, the long stimulus times used made the O2Hb signal particularly susceptible  
 308 to physiological contamination thereby making it less reliable than the HHB signal.<sup>56</sup>

309 Furthermore, the LME results indicate microvascular cerebral hemodynamics may be altered

310 in individuals with bilateral carotid plaques compared with healthy controls in association with an  
311 incongruous Stroop test. Specifically, there appears to be vascular impairment in the Plaque group  
312 compared with the Healthy group; this is demonstrated by a significant reduction in the magnitude  
313 of Hb decrease in the left hemisphere of the brain, which is accompanied by a significantly  
314 reduced increase in O<sub>2</sub>Hb (though the latter is a global effect).

315 Examples of the fNIRS data for individual participants from each group (after temporal pre-  
316 processing but before applying the GLM) are shown in Figure 6. Note the increased magnitude of  
317 the O<sub>2</sub>Hb response globally for the participant in the Healthy group compared with the participant  
318 in the Plaque group. Although smaller in magnitude and not sustained throughout the stimulus, also  
319 note that the drop in Hb in the LPFC for the first 40 seconds during the incongruous condition is  
320 larger in the Healthy participant compared with the Plaque participant (pink arrows).

321 The observation that carotid plaques are associated with a reduction in NVC is similar to previ-  
322 ous studies investigating the effect of atherosclerosis on cerebral hemodynamics and oxygenation.  
323 For example, Khan et. al (2021) used perfusion-weighted MRI to assess the relationship between  
324 carotid stenosis and cerebral perfusion and found that over 80% of patients had a detectable reduc-  
325 tion in brain perfusion in the hemisphere ipsilateral to the carotid stenosis.<sup>57</sup> Lal et. al (2017) used  
326 the transcranial Doppler (TCD) breath-holding index (BHI) to compare cerebral hemodynamics in  
327 patients with asymptomatic carotid stenosis (> 50% occlusion) and age-matched healthy controls,  
328 and found a reduced ipsilateral BHI in half of the patients.<sup>58</sup> Similarly, Vernieri et. al (2006)  
329 demonstrated a significant reduction in vasoreactivity using both fNIRS and TCD in patients with  
330 symptomatic carotid artery occlusion compared to patients with asymptomatic carotid artery oc-  
331 clusion.<sup>59</sup> Furthermore, Forero et. al (2017) used fNIRS to show that patients with carotid stenosis  
332 had (1) a decreased vasoreactivity by 23% and (2) 33% fewer network links in the hemisphere

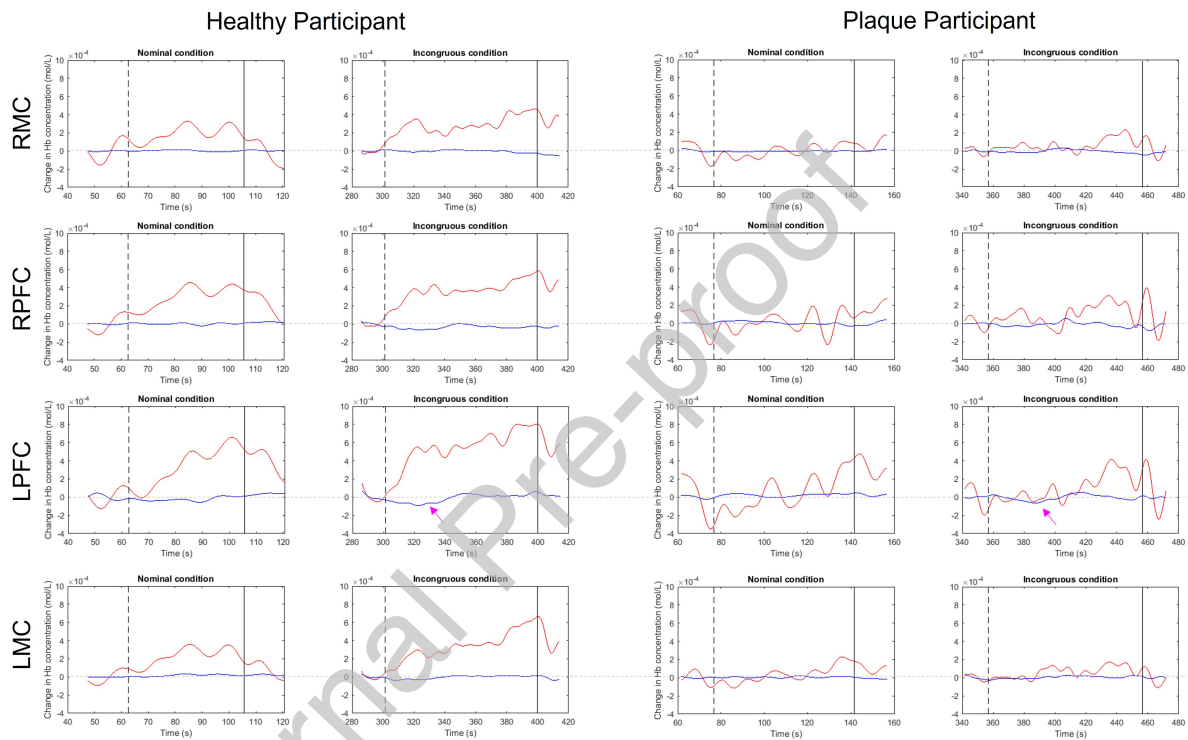


**Fig 6** Example channels from each of the four brain regions assessed for an example participant in the (left) Healthy group and the (right) Plaque group. The Hb signals shown here have been temporally pre-processed as described in Section 2.5.1, but otherwise reflect the raw data (i.e. before short separation channel regression with the GLM). Note that overall, the OHB signal (red lines) increases to a greater extent in response to the incongruous condition for the participant in the Healthy group compared to the participant in the Plaque group. Also note the increased drop in HbB (blue lines) in the LPFC in the Healthy participant compared with the Plaque participant (magenta arrows).



333 ipsilateral to the stenotic vessel.<sup>60</sup> The observation that atherosclerosis is associated with impaired  
334 NVC is further corroborated by Shroeter et. al (2006), who demonstrated that patients with cere-  
335 bral microangiopathy (small vessel disease) had a weaker and delayed hemodynamic response  
336 compared with age-matched controls in both the left and right frontal lobes during a color-word  
337 Stroop task.<sup>61</sup>

338 Given that our study includes only those with bilateral carotid plaques, it is unclear why the  
339 left hemisphere of the brain seems to be more affected than the right. This could be because the  
340 left side plays a more dominant role during the incongruous Stroop task,<sup>53</sup> thus making any deficits  
341 linked to vascular disease in that region more readily apparent. Measurements of plaque size and  
342 carotid intima medial thickness (cIMT) are currently ongoing, and will be used in future work to  
343 further assess the relationship between carotid atherosclerotic burden, plaque characteristics and  
344 cerebral hemodynamics.

345 Interestingly, the observed change in the pattern of brain activation was not accompanied by a  
346 change in central hemodynamic measures or task performance between people with and without  
347 atherosclerosis. Both groups found the incongruous Stroop task similarly 'stressful', and therefore  
348 may have had a similar level of sympathetic nervous system activation. There are several reasons  
349 that could explain the latter observation whereby the Plaque group maintained performance of the  
350 Stroop task despite experiencing reduced NVC in the regions assessed with fNIRS. One expla-  
351 nation could be the nature of the disease progression: hypoperfusion has been shown to *precede*  
352 cognitive decline, and must be chronic and persistent to cause the neuronal energy crisis that trig-  
353 gers neurodegeneration.<sup>8,11</sup> As the participants in the Plaque group had no prior evidence of CVD  
354 and the plaques were found incidentally (i.e. otherwise asymptomatic), we likely identified them  
355 at an early stage of the pathway between altered cerebral hemodynamics and measurable cognitive

356 decline. It is also possible that regions outside of the areas interrogated by fNIRS in this study were  
357 recruited to maintain task performance in a phenomenon referred to as ‘neural compensation’.<sup>62–64</sup>  
358 Working under this supposition, cognitive impairment would then only be apparent when the addi-  
359 tional cognitive reserve were no longer sufficient. Although plausible, this study does not provide  
360 the data support needed to determine whether neural compensation was occurring; this would re-  
361 quire further work using a method capable of measuring global cerebral hemodynamics and neural  
362 activation. Finally, all participants of this study had an MMSE score of 24 or over; if this study  
363 were repeated on participants demonstrating signs of cognitive impairment, a relationship between  
364 hemodynamic measures and task performance might be observed.

365 This study has several limitations. Firstly, the Stroop protocol was designed to be consistent  
366 with a previous INSIGHT wave before the addition of fNIRS. Consequently, the protocol was not  
367 modified to be optimal for fNIRS, which is why each condition in the Stroop test is administered  
368 in a single long block as opposed to multiple short blocks. Although every effort was made to min-  
369 imize the effect of physiological contamination (such as including the short separation channels in  
370 the design matrix and specifying the contrast to compare the incongruous vs. the nominal condi-  
371 tion), we cannot exclude that the cerebral component of the O<sub>2</sub>Hb fNIRS signal is confounded by  
372 extracerebral hemodynamics. Specifically, one concern is the spatial heterogeneity of scalp blood  
373 flow; we used a single short separation channel measurement to reflect the systemic effect for the  
374 entire hemisphere of the head, which is an imperfect method given the variability in systemic blood  
375 flow as a function of location. Although the HbB response is smaller in magnitude, it is less sen-  
376 sitive to this type of contamination (see Figure 7) and thus is likely to be a better indicator of NVC  
377 in this study.<sup>56</sup> This is confirmed by our findings in our ‘known’ condition: we know that there  
378 should be increased activity in the PFC compared to the sensorimotor regions in response to the

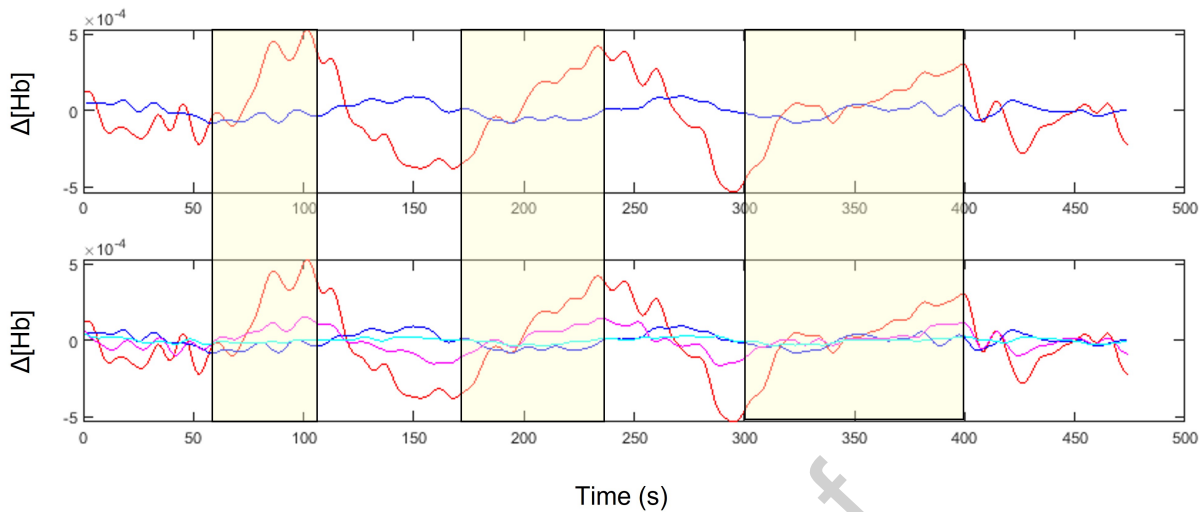


**Fig 7** Top row: Example preprocessed channels from the left prefrontal cortex (LPFC) of a participant in the Healthy group with O2Hb and Hb shown in red and blue respectively. Note that in response to the stimulus periods (yellow blocks), the O2Hb signal increases to a greater extent corresponding decrease in Hb. Bottom row: The same channels as above are duplicated below, this time with the corresponding O2Hb (magenta) and Hb (cyan) measures from the short separation channel superimposed. Note that the O2Hb short separation channel responds in a similar way to the O2Hb long separation channel throughout the Stroop task, whereas the Hb short separation channel maintains a relatively flat shape. This implies that O2Hb is more sensitive to extracerebral contamination than Hb.

379 Stroop task. This was indeed picked up in the Hb signal, which showed a significantly greater  
 380 decrease in Hb concentration on the LPFC than the RMC. However, we would like to emphasize  
 381 that although O2Hb and Hb are not in perfect agreement, they are not necessarily contradictory.  
 382 Rather, the increased concentration of O2Hb in response to the stimulus was more widespread  
 383 whereas the decrease in Hb concentration was more localized. This pattern has been previously  
 384 described in other fNIRS studies.<sup>54</sup>

385 Secondly, we chose to focus on the extremes of atherosclerosis within our sample (no plaques  
 386 vs. bilateral plaques) to increase the chances of detecting differences with a limited sample size.  
 387 In future it would be valuable to examine the relationship between NVC and atherosclerosis using  
 388 atherosclerosis as a graded rather than a binary measure, although this is likely to require a larger  
 389 sample size.

390 Although the Plaque and Healthy groups were age-matched and had relatively similar cardio-  
391 vascular health profiles with the exception of the presence of carotid plaques, there was a difference  
392 in numbers of men between the two groups (70% men in the Plaque group versus 36% men in the  
393 Healthy group). We performed an additional LME analysis with statistical adjustment for sex (see  
394 supplementary information S2) and saw little effect on the overall results, but the sample size used  
395 was too small to draw any firm conclusions regarding the influence of sex on observed associ-  
396 ations. Lastly, the sample was drawn from a UK-based national birth cohort and only included  
397 people of White European ethnicity and consequently our findings may not be generalizable to  
398 other samples.

399 This study also has many strengths which are worth highlighting. Firstly, we were able to  
400 take advantage of the advanced fNIRS preprocessing methods offered by SPM-fNIRS, such as  
401 customizing our design matrix to include physiological contaminants, and using pre-whitening  
402 to correct for serial autocorrelations in our data. Both of these have the effect of reducing the  
403 false positive rate, thereby giving us confidence that our results are robust even in the presence of  
404 noise. The Polhemus digitization and statistical parametric mapping also enabled us to preserve the  
405 geometry of of our fNIRS measurements such that we could perform our analyses on anatomical  
406 regions rather than being restricted to channel-wise analyses. Secondly the extensive phenotyping  
407 performed as part of this study and previous data acquired as part of the NSHD enabled us to  
408 compare health and cognition status between our groups: this gives us some confidence that the  
409 differences observed in the cerebral hemodynamics between the two groups are likely to be a  
410 reflection of the differences related to carotid atherosclerosis.

## 411 **5 Conclusions**

412 As expected, evidence of brain activation based on fNIRS measurement of HHB was found in the  
413 LPFC of all participants. Despite individual heterogeneity of brain activation patterns, a consistent  
414 decrease in brain activity was observed in participants with bilateral carotid plaques compared with  
415 healthy controls during the incongruous Stroop task. Interestingly, this change in activation pattern  
416 was not accompanied by a marked differences in MAP, HR, or task performance. We demonstrate  
417 that carotid atherosclerosis, a well-established cardiovascular risk factor, may be associated with  
418 alterations in NVC while performing the Stroop task even in the absence of detectably impaired  
419 cognitive performance.

## 420 **Funding**

421 Insight 46 is funded by grants from Alzheimer's Research UK (ARUK-PG2014-1946, ARUK-  
422 PG2017-1946 PIs Schott, Fox, Richards), the Medical Research Council Dementias Platform UK  
423 (CSUB19166 PIs Schott, Fox, Richards), the Wolfson Foundation (PR/ylr/18575 PIs Fox, Schott),  
424 the Medical Research Council (MC\_UU\_12019/1 PI Kuh and MC\_UU\_12019/3 PI Richards), the  
425 Wellcome Trust (Clinical Research Fellowship 200109/Z/15/Z Parker) and Brain Research Trust  
426 (UCC14191, PI Schott). The cardiovascular assessments of Insight 46 are funded by a grant from  
427 the British Heart Foundation (PG17/90/33415 PI Hughes). Hughes also receives support from  
428 the British Heart Foundation, the Economic and Social Research Council (ESRC), the Horizon  
429 2020 Framework Programme of the European Union, the National Institute on Aging, the National  
430 Institute for Health Research University College London Hospitals Biomedical Research Centre,  
431 the UK Medical Research Council.

## 432 **Acknowledgments**

433 We would like to thank the study members from the MRC National Survey of Health and Devel-  
434 opment (NSHD) for their lifelong commitment to the study and the Insight 46 and NSHD study  
435 teams for their work, help and guidance.

## 436 **Disclosures**

437 Nish Chaturvedi serves on a Data Safety and Monitoring Board for a clinical trial of a glucose  
438 lowering agent, funded by AstraZeneca. No other authors have competing interests.

## 439 *References*

- 440 1 E. B. Mathiesen, K. Waterloo, O. Joakimsen, *et al.*, “Neuropsychological Test Performance  
441 in Asymptomatic Carotid Stenosis,” *Acta Neurologica Scandinavica* **107**(6), 427–428 (2003).
- 442 2 A. Kearney-Schwartz, P. Rossignol, S. Bracard, *et al.*, “Vascular Structure and Function Is  
443 Correlated to Cognitive Performance and White Matter Hyperintensities in Older Hyperten-  
444 sive Patients With Subjective Memory Complaints,” *Stroke* **40**(4), 1229–1236 (2009).
- 445 3 B. Sabayan, M. A. van Buchem, S. Sigurdsson, *et al.*, “Cardiac hemodynamics are linked with  
446 structural and functional features of brain aging: the age, gene/environment susceptibility  
447 (AGES)-Reykjavik Study,” *Journal of the American Heart Association* **4**(1), e001294 (2015).
- 448 4 J. R. Romero, A. Beiser, S. Seshadri, *et al.*, “Carotid artery atherosclerosis, MRI indices  
449 of brain ischemia, aging, and cognitive impairment: The framingham study,” *Stroke* **40**(5),  
450 1590–1596 (2009).
- 451 5 R. D. Bell and B. V. Zlokovic, “Neurovascular mechanisms and blood-brain barrier disorder  
452 in Alzheimer’s disease,” *Acta Neuropathologica* **118**(1), 103–113 (2009).

- 453 6 M. M. B. Breteler, “Vascular risk factors for Alzheimer’s disease: An epidemiologic perspec-  
454 tive,” *Neurobiology of Aging* **21**, 153–160 (2000).
- 455 7 J. C. De La Torre, “Cardiovascular risk factors promote brain hypoperfusion leading to cog-  
456 nitive decline and dementia,” *Cardiovascular Psychiatry and Neurology* **2012** (2012).
- 457 8 K. Honjo, S. E. Black, and N. P. L. G. Verhoeff, “Alzheimer’s Disease, Cerebrovascular  
458 Disease, and the  $\beta$ -amyloid Cascade,” *Canadian Journal of Neurological Sciences / Journal*  
459 *Canadien des Sciences Neurologiques* **39**(6), 712–728 (2012).
- 460 9 J. C. Kovacic, J. M. Castellano, and V. Fuster, “The links between complex coronary disease,  
461 cerebrovascular disease, and degenerative brain disease,” *Annals of the New York Academy of*  
462 *Sciences* **1254**(1), 99–105 (2012).
- 463 10 J. C. de la Torre and T. Mussivand, “Can disturbed brain microcirculation cause Alzheimer’s  
464 disease?,” *Neurol Res* **15**(3), 146 – 153 (1993).
- 465 11 J. de la Torre, “The Vascular Hypothesis of Alzheimer’s Disease: A Key to Preclinical Predic-  
466 tion of Dementia Using Neuroimaging,” *Journal of Alzheimer’s disease : JAD* **63**(1), 35–52  
467 (2018).
- 468 12 A. A. Rensink, R. M. De Waal, B. Kremer, *et al.*, “Pathogenesis of cerebral amyloid angiopa-  
469 thy,” *Brain Research Reviews* **43**(2), 207–223 (2003).
- 470 13 A. Hofman, A. Ott, M. M. Breteler, *et al.*, “Atherosclerosis, apolipoprotein E, and prevalence  
471 of dementia and Alzheimer’s disease in the Rotterdam Study,” *Lancet* **349**(9046), 151–154  
472 (1997).
- 473 14 L. S. Honig, W. Kukull, and R. Mayeux, “Atherosclerosis and AD Analysis of data from the  
474 US National Alzheimer ’ s,” *Neurology* **64**, 494 – 500 (2005).

- 475 15 L. Li, D. Cao, D. W. Garber, *et al.*, “Association of Aortic Atherosclerosis with Cerebral  
476  $\beta$ -Amyloidosis and Learning Deficits in a Mouse Model of Alzheimer’s Disease,” *American*  
477 *Journal of Pathology* **163**(6), 2155–2164 (2003).
- 478 16 D. Kuh, M. Pierce, J. Adams, *et al.*, “Cohort Profile: Updating the cohort profile for the MRC  
479 National Survey of Health and Development: A new clinic-based data collection for ageing  
480 research,” *International Journal of Epidemiology* **40**(1) (2011).
- 481 17 S. N. James, C. A. Lane, T. D. Parker, *et al.*, “Using a birth cohort to study brain health  
482 and preclinical dementia: Recruitment and participation rates in Insight 46,” *BMC Research*  
483 *Notes* **11**(1), 1–9 (2018).
- 484 18 D. Kuh, A. Wong, I. Shah, *et al.*, “The MRC National Survey of Health and Development  
485 reaches age 70: maintaining participation at older ages in a birth cohort study,” *European*  
486 *Journal of Epidemiology* **31**(11), 1135–1147 (2016).
- 487 19 C. A. Lane, T. D. Parker, D. M. Cash, *et al.*, “Study protocol: Insight 46 - a neuroscience  
488 sub-study of the MRC National Survey of Health and Development,” *BMC Neurology* **17**(1),  
489 1–25 (2017).
- 490 20 S. A. Mason, L. Al Saikhan, S. Jones, *et al.*, “Study Protocol - Insight 46 Cardiovascular:  
491 A Sub-study of the MRC National Survey of Health and Development,” *Artery Research*  
492 (2020).
- 493 21 M. Prince, E. Albanese, M. Guerchet, *et al.*, “World Alzheimer Report 2014,” tech. rep.,  
494 Alzheimer’s Disease International, London (2014).
- 495 22 F. Scholkmann, S. Kleiser, A. J. Metz, *et al.*, “A review on continuous wave functional near-



- 496 infrared spectroscopy and imaging instrumentation and methodology.,” *NeuroImage* **85 Pt 1**,  
497 6–27 (2014).
- 498 23 S. C. Bunce, M. Izzetoglu, K. Izzetoglu, *et al.*, “Functional near-infrared spectroscopy,” *IEEE*  
499 *Engineering in Medicine and Biology Magazine* **25**(4), 54–62 (2006).
- 500 24 P. Pinti, A. Merla, C. Aichelburg, *et al.*, “A novel GLM-based method for the Automatic  
501 IDentification of functional Events (AIDE) in fNIRS data recorded in naturalistic environ-  
502 ments,” *NeuroImage* **155**(May), 291–304 (2017).
- 503 25 C. Udina, S. Avtzi, T. Durduran, *et al.*, “Functional Near-Infrared Spectroscopy to Study  
504 Cerebral Hemodynamics in Older Adults During Cognitive and Motor Tasks: A Review,”  
505 *Frontiers in Aging Neuroscience* **11**(January), 1–19 (2020).
- 506 26 J. R. Stroop, “Studies of interference in serial verbal reactions,” *Journal of Experimental*  
507 *Psychology* **18**(6), 643–662 (1935).
- 508 27 F. Scarpina and S. Tagini, “The stroop color and word test,” *Frontiers in Psychology* **8**(APR),  
509 1–8 (2017).
- 510 28 P. Vendrell, C. Junqué, J. Pujol, *et al.*, “The role of prefrontal regions in the Stroop task,”  
511 *Neuropsychologia* **33**(3), 341–352 (1995).
- 512 29 D. J. Davidson, R. T. Zacks, and C. C. Williams, “Stroop Interference, Practice, and Aging,”  
513 *Aging, Neuropsychology, and Cognition* **10**(2), 85–98 (2003).
- 514 30 H. Amieva, S. Lafont, I. Rouch-Leroyer, *et al.*, “Evidencing inhibitory deficits in Alzheimer’s  
515 disease through interference effects and shifting disabilities in the Stroop test,” *Archives of*  
516 *Clinical Neuropsychology* **19**(6), 791–803 (2004).

- 517 31 M. Laguë-Beauvais, J. Brunet, L. Gagnon, *et al.*, “A fNIRS investigation of switching and  
518 inhibition during the modified Stroop task in younger and older adults,” *NeuroImage* (2013).
- 519 32 D. H. Spieler, D. A. Balota, and M. E. Faust, “Stroop Performance in Healthy Younger and  
520 Older Adults and in Individuals with Dementia of the Alzheimer’s Type,” *Journal of Experi-  
521 mental Psychology: Human Perception and Performance* **22**(2), 461–479 (1996).
- 522 33 R. Hardy, A. K. Ghosh, J. Deanfield, *et al.*, “Birthweight, childhood growth and left ven-  
523 tricular structure at age 6064 years in a British birth cohort study,” *International Journal of  
524 Epidemiology* **45**(4), 1091–1102 (2016).
- 525 34 P. J. Touboul, M. G. Hennerici, S. Meairs, *et al.*, “Mannheim carotid intima-media thickness  
526 and plaque consensus (2004-2006-2011),” *Cerebrovascular Diseases* **34**(4), 290–296 (2012).
- 527 35 V. Jurcak, D. Tsuzuki, and I. Dan, “10/20, 10/10, and 10/5 systems revisited: Their validity  
528 as relative head-surface-based positioning systems,” *NeuroImage* **34**(4), 1600–1611 (2007).
- 529 36 S. Tak, M. Uga, G. Flandin, *et al.*, “Sensor space group analysis for fNIRS data,” *Journal of  
530 Neuroscience Methods* **264**, 103–112 (2016).
- 531 37 F. Scholkmann and M. Wolf, “General equation for the differential pathlength factor of the  
532 frontal human head depending on wavelength and age,” *Journal of Biomedical Optics* **18**(10),  
533 105004 (2013).
- 534 38 F. Scholkmann, S. Spichtig, T. Muehlemann, *et al.*, “How to detect and reduce movement  
535 artifacts in near-infrared imaging using moving standard deviation and spline interpolation,”  
536 *Physiological Measurement* **31**(5), 649–662 (2010).
- 537 39 M. A. Yücel, A. v. Lühmann, F. Scholkmann, *et al.*, “Best practices for fNIRS publications,”  
538 *Neurophotonics* **8**(01), 1–34 (2021).

- 539 40 T. J. Huppert, “Commentary on the statistical properties of noise and its implication on gen-  
540 eral linear models in functional near-infrared spectroscopy,” *NeuroPhotonics* **3**(1), 010401  
541 (2016).
- 542 41 K. J. Friston, D. E. Glaser, R. N. Henson, *et al.*, “Classical and Bayesian inference in neu-  
543 roimaging: Applications,” *NeuroImage* **16**(2), 484–512 (2002).
- 544 42 P. L. Purdon and R. M. Weisskoff, “Effect of temporal autocorrelation due to physiologi-  
545 cal noise and stimulus paradigm on voxel-level false-positive rates in fMRI,” *Human Brain*  
546 *Mapping* **6**(4), 239–249 (1998).
- 547 43 Martin A. Lindquist, Ji Meng Loh, Lauren Y. Atlas, *et al.*, “Modeling the Hemodynamic  
548 Response Function in fMRI: Efficiency, Bias and Mis-modeling,” *Neuroimage* **45**(212), 187–  
549 198 (2009).
- 550 44 M. A. Yücel, J. Selb, C. M. Aasted, *et al.*, “Short separation regression improves statistical  
551 significance and better localizes the hemodynamic response obtained by near-infrared spec-  
552 troscopy for tasks with differing autonomic responses,” *NeuroPhotonics* **2**(3), 035005 (2015).
- 553 45 I. N. Beratis, A. Rabavilas, G. N. Papadimitriou, *et al.*, “Effect of handedness on the Stroop  
554 colour word task,” *Laterality* **15**(6), 597–609 (2010).
- 555 46 C. Li, J. Zheng, J. Wang, *et al.*, “An fMRI Stroop Task Study of Prefrontal Cortical Function  
556 in Normal Aging, Mild Cognitive Impairment, and Alzheimers Disease,” *Current Alzheimer*  
557 *Research* **6**(6), 525–530 (2009).
- 558 47 M. P. Milham, K. I. Erickson, M. T. Banich, *et al.*, “Attentional control in the aging brain:  
559 Insights from an fMRI study of the stroop task,” *Brain and Cognition* **49**(3), 277–296 (2002).
- 560 48 K. U. o. C. Cuevas, G. Calkins, Susan D. (University of North Carolina, and M. A. V. T.

- 561 Bell, “To Stroop or Not to Stroop: Sex-Related Differences in Brain-Behavior Associations  
562 During Early Childhood,” *Psychophysiology* **53**(1) (2016).
- 563 49 K. L. Roberts and D. A. Hall, “Examining a supramodal network for conflict processing: A  
564 systematic review and novel functional magnetic resonance imaging data for related visual  
565 and auditory stroop tasks,” *Journal of Cognitive Neuroscience* **20**(6), 1063–1078 (2008).
- 566 50 A. R. Laird, K. M. McMillan, J. L. Lancaster, *et al.*, “A comparison of label-based review  
567 and ALE meta-analysis in the stroop task,” *Human Brain Mapping* **25**(1), 6–21 (2005).
- 568 51 M. A. Vanderhasselt, R. de Raedt, and C. Baeken, “Dorsolateral prefrontal cortex and Stroop  
569 performance: Tackling the lateralization,” *Psychonomic Bulletin and Review* **16**(3), 609–612  
570 (2009).
- 571 52 S. Zysset, K. Müller, G. Lohmann, *et al.*, “Color-Word Matching Stroop task: Separating  
572 interference and response conflict,” *NeuroImage* **13**(1), 29–36 (2001).
- 573 53 J. Jonides, C. Marshuetz, E. E. Smith, *et al.*, “Age differences in behavior and PET activation  
574 reveal differences in interference resolution in verbal working memory,” *Journal of Cognitive  
575 Neuroscience* **12**(1), 188–196 (2000).
- 576 54 P. Pinti, M. F. Siddiqui, A. D. Levy, *et al.*, “An analysis framework for the integration of  
577 broadband NIRS and EEG to assess neurovascular and neurometabolic coupling,” *Scientific  
578 Reports* **11**(1), 1–20 (2021).
- 579 55 M. L. Schroeter, S. Zysset, F. Kruggel, *et al.*, “Age dependency of the hemodynamic response  
580 as measured by functional near-infrared spectroscopy,” *NeuroImage* **19**(3), 555–564 (2003).
- 581 56 I. Tachtsidis and F. Scholkmann, “Publisher’s note: False positives and false negatives in

- 582 functional near-infrared spectroscopy: issues, challenges, and the way forward,” *Neuropho-*  
583 *tonics* **3**(3), 039801 (2016).
- 584 57 A. A. Khan, J. Patel, S. Desikan, *et al.*, “Asymptomatic carotid artery stenosis is associated  
585 with cerebral hypoperfusion,” *Journal of Vascular Surgery* **73**(5), 1611–1621.e2 (2021).
- 586 58 B. K. Lal, M. C. Dux, S. Sikdar, *et al.*, “Asymptomatic carotid stenosis is associated with  
587 cognitive impairment,” *Journal of Vascular Surgery* **66**(4), 1083–1092 (2017).
- 588 59 F. Vernieri, M. Silvestrini, F. Tibuzzi, *et al.*, “Hemoglobin oxygen saturation as a marker of  
589 cerebral hemodynamics in carotid artery occlusion: An integrated transcranial doppler and  
590 near-infrared spectroscopy study,” *Journal of Neurology* **253**(11), 1459–1465 (2006).
- 591 60 E. Forero, S. Novi, W. Avelar, *et al.*, “Use of near-infrared spectroscopy to probe occlu-  
592 sion severity in patients diagnosed with carotid atherosclerotic disease,” *Medical Research*  
593 *Archives* **5**(6) (2017).
- 594 61 M. L. Schroeter, S. Cutini, M. M. Wahl, *et al.*, “Neurovascular coupling is impaired in cere-  
595 bral microangiopathy—An event-related Stroop study,” *NeuroImage* **34**(1), 26–34 (2007).
- 596 62 M. N. Braskie, G. W. Small, and S. Y. Bookheimer, “Vascular health risks and fMRI activation  
597 during a memory task in older adults,” *Neurobiology of Aging* **31**(9), 1532–1542 (2010).
- 598 63 M. W. Bondi, W. S. Houston, L. T. Eyler, *et al.*, “fMRI evidence of compensatory mechanisms  
599 in older adults at genetic risk for Alzheimer Disease,” *Neurology* **64**(3), 501–508 (2005).
- 600 64 H. Wishart, “Increased Brain Activation During Working Memory in Cognitively Intact  
601 Adults With the APOE  $\epsilon$ 4 Allele,” *American Journal of Psychiatry* **163**(9), 1603 (2006).

**Credit Author Statment**

Sarah A Mason: Conceptualization, Writing - Original draft preparation, software, Formal analysis, Visualization,

Lamia Al Saikhan: Writing - review & editing, Investigation,

Siana Jones: Writing - review & editing, Investigation,

Sarah-Naomi James: Writing - review & editing, Data curation,

Heidi Murray-Smith: Investigation, Project administration,

Alicja Rapala: Project administration,

Suzanne Williams: Investigation,

Carole Sudre: software, Writing - review & editing, Data curation,

Brian Wong: Investigation,

Marcus Richards: Writing - review & editing, Funding acquisition

Nick C. Fox Writing - review & editing, Funding acquisition,

Rebecca Hardy, Writing - review & editing, Funding acquisition,

Jonathan M. Schott: Writing - review & editing, Funding acquisition,

Nish Chaturvedi: Writing - review & editing, Funding acquisition,

Alun D Hughes Conceptualization, Supervision, Formal analysis, Writing - review & editing, Funding acquisition.